DPC AND DTC CONTROL OF A VARIABLE WIND SPEED BASED ON DOUBLE FED ASYNCHRONOUS MACHINE

A.Moualdia **MO. Mahmoudi**
Process Control Laboratory, Ecole National Polytechnique
BP. 182, 16200 El-Harrach, Algiers, Algeria
amoualdia1@yahoo.fr
L. Nezli
Process Control Laboratory, Ecole National Polytechnique
BP. 182, 16200 El-Harrach, Algiers, Algeria

Abstract *- This paper proposes two techniques to control DTC (Direct Torque Control) and DPC (Direct Power Control), applied to the system of converting wind energy with a double-fed asynchronous machine. Conventionally, the DTC is developed from the expressions of the model of DFIG in the reference connected to the rotor, so the amplitude of the flux is estimated from the voltages and currents of the rotor. The reference torque is obtained by a mechanical speed controller of the machine whose goal is to have a maximum power point tracking (MPPT). On the other hand, the DPC is achieved while using a new switching table without sensor voltage. The instantaneous active and reactive power is controlled directly by selecting the optimum condition of the network side converter. The main objective of the control system and maintain the DC bus voltage level required. Consequently, the input currents from the network should be sinusoidal and in phase with the voltages to meet operating at unity power factor. The results obtained show the interest of both techniques.*

Key words: *Asynchronous machine, PWM converters, Direct torque control, direct power control, Wind generator, MPPT.*

1. Introduction

Today, wind energy has become an inescapable reality world. The evolution of the capacity of electricity generation by wind turbines has been increasing since 1980. The wind industry is capable of becoming a global energy industry if it is based on the acceleration of facilities in the last decade. The wind energy can contribute a significant share of new energy sources that do not emit greenhouse gas emissions. Their rational exploitation to produce electricity. These theoretically exploitable renewable energy are numerous and varied.

The development of wind energy has grown significantly due to the diversity of exploitable areas relatively attractive and cost [1]. Wind energy systems are growing more quickly because we can now rely on proven and reliable techniques. Moreover, the energy potential of global energy is estimated at an output of 5300 TWh, which represents a significant energy deposit and very promising [2]. Much of the wind turbines installed today are equipped with double-fed induction machine (DFIG). This generator provides electricity generation, variable speed; this allows them to better exploit the wind resources for different wind conditions. These turbines are also equipped with propeller blade pitch to accommodate variable wind conditions. The entire turbine is controlled to maximize the power produced continuously seeking the operating point at maximum power commonly called MPPT. However, this type of energy is an energy booster from nuclear generation remains largely predominant.

The induction motor squirrel cage has been widely used as generator in wind turbines [2]. Indeed, it is robust, inexpensive and simple to implement. In contrast, most of these machines are connected

Directly to the network to avoid the presence of a converter. This direct connection requires operation at fixed speed and therefore, limited effectiveness in high wind speeds. The double-fed induction machine (DFIG), even if it has a less robust wound rotor and sliding contacts, is used to allow variable speed operation of ± 30% around the synchronous speed [3-4-5]. The stator is directly connected to the network and the rotor is connected to the network via a bidirectional converter. This converter is scaled to deal with 30% of the nominal power of the machine. For higher speeds the timing, if the converter is reversible, the machine can also produce energy from the rotor to the network up to 0.3 times rated power. Overall, in the best case, the machine can deliver 1.3 times its rated power. To be able to test the laws regulating a wind system, it appears necessary to have a simulation tool capable of modeling the entire chain of energy conversion and predict its performance. Initially, a model of wind generator was proposed in Matlab / Simulink to evaluate its dynamic performance in these different operating conditions. Then, we present two techniques DTC control and DPC respectively applied to the DFIG machine of 7.5 kw and side PWM converter system.

2. Wind generator modeling

2.1. Modélisation of the turbine

The overall pattern of a string conversion of wind energy connected to the grid is described in Figure 1

Figure.1. Diagram of a chain of energy conversion

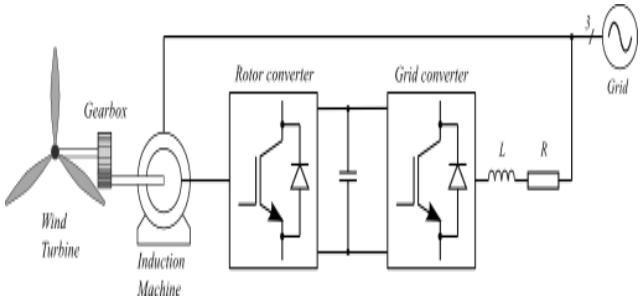

Figure.1. Diagram of a chain of energy conversion

The mechanical power available on the shaft of a wind turbine is expressed by the equation:

$$P_m = 0.5C_p(\lambda)\pi\rho R^2 V_1^3 \qquad (1)$$

The power coefficient C_p is the aerodynamic efficiency of the wind turbine. It depends on the characteristic of the turbine. The variation coefficient as a function of speed ratio λ and angle of orientation of the blade β.

$$C_p = f(\lambda,\beta) = C_1\left(\frac{C_2}{\lambda_i} - C_3 - C_4\right)\exp\left(\frac{-C_5}{\lambda_i}\right) + C_6\lambda \qquad (2)$$

With

$$\frac{1}{\lambda_i} = \frac{1}{\lambda + 0.08\beta} - \frac{0.035}{\beta^3 + 1}; \qquad (3)$$

C_1=0.5176, C_2=116, C_3=0.4, C_4=5, C_5=21, C_6=0.0068;

and β: the angle of the blades; The speed ratio λ is defined as the ratio between the linear speed of the blades and the wind speed $\lambda = \frac{R.\Omega_1}{V}$ with V: wind speed, Ω1: mechanical angular speed of the turbine

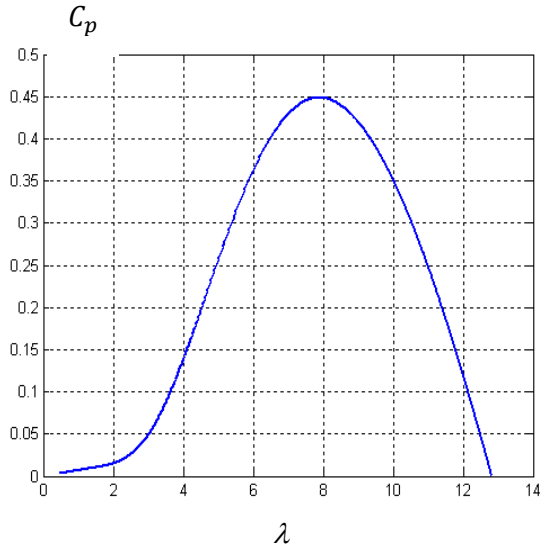

Figure.2. Power coefficient

The variation of mechanical power based on the rotational speed of the generator for different wind speeds is illustrated in Figure 3.

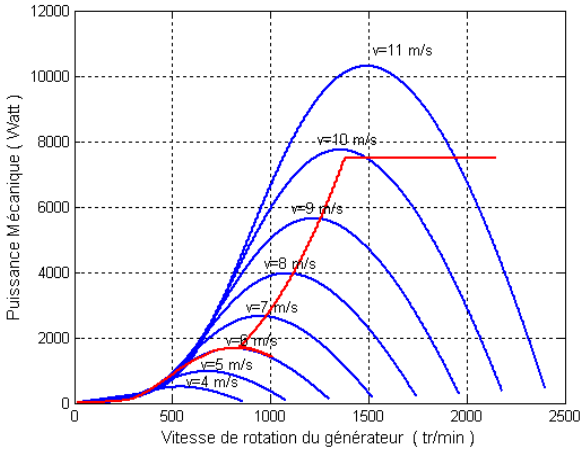

Figure.3. Mechanical power

2.2. Modélisation generator

The generator chosen for the conversion of wind energy is a double-fed induction generator, DFIG modeling described in the repository of Park, is presented by the system of equations:

$$\begin{cases} V_{sd} = R_s i_{sd} + \dfrac{d\varphi_{sd}}{dt} - \dot{\theta}_s \varphi_{sq} \\ V_{sq} = R_s i_{sq} + \dfrac{d\varphi_{sq}}{dt} + \dot{\theta}_s \varphi_{sd} \\ V_{rd} = R_r i_{rd} + \dfrac{d\varphi_{rd}}{dt} - \dot{\theta}_r \varphi_{rq} \\ V_{rq} = R_r i_{rq} + \dfrac{d\varphi_{rq}}{dt} + \dot{\theta}_r \varphi_{rd} \end{cases} \quad (4)$$

$$\begin{cases} \varphi_{sd} = L_s i_{sd} + M i_{rd} \\ \varphi_{sq} = L_s i_{sq} + M i_{rq} \\ \varphi_{rd} = L_r i_{rd} + M i_{sd} \\ \varphi_{rq} = L_r i_{rq} + M i_{sd} \end{cases} \quad (5)$$

$$C_{em} = \frac{pM}{L_s}\left(\varphi_{sd} i_{rq} - \varphi_{sq} i_{rd}\right) \quad (6)$$

$$C_{éolien} = C_{em} + f.\Omega + J\frac{d\Omega}{dt} \quad (7)$$

In the two-phase marker, the stator active and reactive power of asynchronous generator written:

$$\begin{cases} P_s = V_{sd}.i_{sd} + V_{sq}.i_{sq} \\ Q_s = V_{sq}.i_{sd} - V_{sd}.i_{sq} \end{cases} \quad (8)$$

2.3. Maximisation MPPT power by sliding mode

The techniques for extracting the maximum power are to determine the speed of the turbine which achieves maximum power output. The reference speed of the turbine corresponds to that corresponding to the optimal value of speed ratio (at β constant and equal to 0 °) to obtain the maximum value of (Cp = 0.47). This command structure is to adjust the torque shown on the turbine shaft so as to determine its speed at its reference written by $\Omega_{tur-ref} = \frac{\lambda_{opt}.V}{R}$. To adjust the speed was used to sliding mode control; it was a great success in recent years. This is due to the simplicity of implementation and robustness against system uncertainties and external disturbances marring the process. The sliding mode control is to reduce the state trajectory toward the sliding surface and make it evolve over a certain dynamic to the equilibrium point [6-7]. The design of sliding mode control returns to identify three stages.

2.3.1. Choix surface switching

For a nonlinear system presented in the following form

$$\dot{X} = f(X,t) + g(X,t).u(X,t) X \in \mathcal{R}, u \in \mathcal{R} \quad (9)$$

Where $f(X,t), g(X,t)$ both functions are continuous and nonlinear uncertain assumed bounded. It takes the form of general equation proposed by J.J. Slotine to determine the sliding surface given by: [8]

$$S(X) = \left(\frac{d}{dt} + \gamma\right)^{n-1} .e \quad (10)$$

$$e = X^d - X \quad (11)$$

With

$X = [x, \dot{x}, \ldots x^{n-1}]^T , X^d = [x^d, \dot{x}^d, \ldots]^T$

and e: error on the variable to be controlled

γ: coefficient positive-n-order system X d: X size desired: state variable of the quantity ordered.

2.3.2. Condition convergence

The convergence condition is defined by the Lyapunov equation; it makes the area attractive and invariant.

$$(S(X))\left(S(\dot{X})\right) \leq 0 \quad (12)$$

2.3.3. Calcul control

The control algorithm is defined by the relation

$$u = u^{eq} + u^{n} \quad (13)$$

$$u^{n} = \frac{u^{max} sat(S(X))}{\emptyset} \quad (14)$$

$$sat\left(\frac{S(X)}{\emptyset}\right) = \begin{cases} sign(s) & si \ |s| > \emptyset \\ \frac{s}{\emptyset} & si \quad |s| < \emptyset \end{cases} \quad (15)$$

With: u: manipulated variable,u^{eq}: equivalent control magnitude, u^{n}: switching control term, sat (S (X)) / φ: saturation function,

φ: width of the threshold of saturation functions

2.4. Control speed

To control speed we take n = 1, the expression of the control surface of the angular velocity of the machine has the form:

$$S(\Omega) = \Omega_{ref} - \Omega \quad (16)$$

During the sliding mode and steady we have:

$$\dot{S}(\Omega) = 0 \Rightarrow \dot{S}(\Omega) = 0 \Rightarrow Cem_{eq} = C_{turbine} + f.\Omega \quad (17)$$

During the mode of convergence we have:

$$S(\Omega).\dot{S}(\Omega) < 0 \Rightarrow Cem_{n} = \begin{cases} \left({}^{K_\Omega}/_{\emptyset_\Omega}\right).S(\Omega) \ si \ S(\Omega) < \emptyset_\Omega \\ K_\Omega Sign\left(S(\Omega)\right) \ si \ S(\Omega) > \emptyset_\Omega \end{cases} \quad (18)$$

The structure of maximizing power (MPPT) by the sliding mode controller has been simulated by considering a wind profile using (10m/s) (Figure 4) The results corresponding to this strategy show that variations in the speed of DFIG are adapted to the change in wind speed, the performance of sliding mode control are very satisfactory with a good pursuit of the reference. The ratio of the speed and power coefficient are adjusted 8.1, 0447 respectively to their maximum value

3. Direct torque control (DTC) of the DFIG

The Direct Torque Control (figure 5) is based on flow control and torque control using hysteresis. The rotor flux is estimated from the equation of the DFIG rotor voltage:

$$\frac{d\overline{\psi r}}{dt} = \overline{Vr} - Rr.\overline{Ir} \quad (19)$$

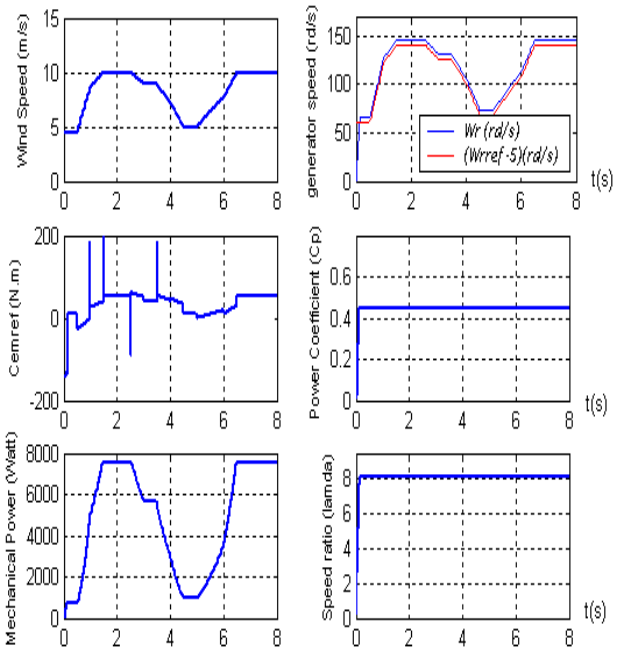

Figure.4. Command performances for MPPT

In the $\alpha\beta$ reference, the rotor flux components are determined as follows:

$$\begin{cases} \psi_{r\alpha} = \int (V_{r\alpha} - R_r.I_{r\alpha})\, dt \\ \psi_{r\beta} = \int (V_{r\beta} - R_r.I_{r\beta})\, dt \end{cases} \quad (20)$$

$$\psi_r = \sqrt{\psi_{r\alpha}^2 + \psi_{r\beta}^2} \quad (21)$$

$$\hat{\theta}r = arccos\left({}^{\psi_{r\alpha}}/_{\psi_r}\right) \quad (22)$$

The electromagnetic torque is estimated as

$$Cem_{est} = p.\left(\psi_{r\alpha} I_{r\beta} - \psi_{r\beta} I_{r\alpha}\right) \quad (23)$$

The switching table given below is constructed in the state variables e_ψ , e_c and sector N position of ψ_r.

	N	1	2	3	4	5	6
$e_\psi = 1$	$e_c = 1$	V_2	V_3	V_4	V_5	V_6	V_1
	$e_c = 0$	V_7	V_0	V_7	V_0	V_7	V_0
	$e_c = -1$	V_6	V_1	V_2	V_3	V_4	V_5
$e_\psi = 0$	$e_c = 1$	V_3	V_4	V_5	V_6	V_1	V_2
	$e_c = 0$	V_0	V_7	V_0	V_7	V_0	V_7
	$e_c = -1$	V_5	V_6	V_1	V_2	V_3	V_4

Table 1.Table switching

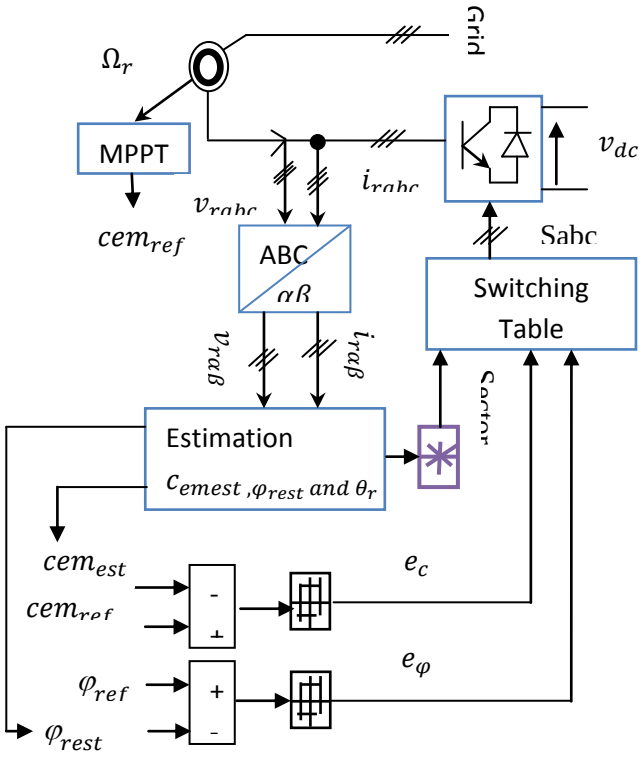

Figure .5 .Structure of the DTC for the DFIG

With V0= [000] ; V1= [100] ; V2= [110] ;
V3= [010] ; V4= [011] V5= [001] ;
V6= [101] ; V7= [111]

The vectors V0 and V7 are selected alternately to minimize the number of switching into the arms of the inverter.

4. Direct control of power for the grid side converter

The principle of the DPC Figure 6 is based on the control loops of instantaneous active and reactive powers. In DPC there is no inner loop power. The switching states of the converter are selected by the switching table; the latter is made from the instantaneous errors obtained from the difference between the estimated and measured power (active and reactive). To order the relay functionality using two hysteresis comparators and a switching table [9-10-11]. In this configuration the DC bus voltage regulator is controlled by a conventional PI (proportional-integrator), the latter providing the reference active power P_{ref} and the reference reactive power (Q_{ref}= 0) is kept zero in order have an operation at unity power factor. Errors obtained from the difference are applied as inputs to comparator hysteresis and scan for signals Sp, Sq The position of voltage vector is used to determine the area N.

$(N-2)\frac{\pi}{6} \le \theta_e \le (N-1)\frac{\pi}{6}$, N=1, 2, 3..., 12

The digitized signals Sp, Sq and n are considered inputs to the switching table in which each switching state, ka, kb and kc, the converter is stored. Using this switching table, the optimal state switching converter can be selected in any single specific times depending on the combination of input signals.

4.1. Modeling System

In the fixed plane and a three-phase balanced phase currents can be presented as follows:

$$\begin{cases} \frac{di_\alpha}{dt} = \frac{1}{L}(e_\alpha - v_\alpha - R.i_\alpha) \\ \frac{di_\beta}{dt} = \frac{1}{L}(e_\beta - v_\beta - R.i_\beta) \end{cases} \quad (24)$$

The resistance parameter R can be virtually neglected and a discrete approximation of equation (16) can be adopted. Thus the change in the current stage for a sampling period is given by:

$$\Delta i_\alpha = i_\alpha(k+1) - i_\alpha(k) = \frac{T_S}{L}\left(e_\alpha(k) - v_\alpha(k)\right) \quad (25)$$

$$\Delta i_\beta = i_\beta(k+1) - i_\beta(k) = \frac{T_S}{L}\left(e_\beta(k) - v_\beta(k)\right) \quad (26)$$

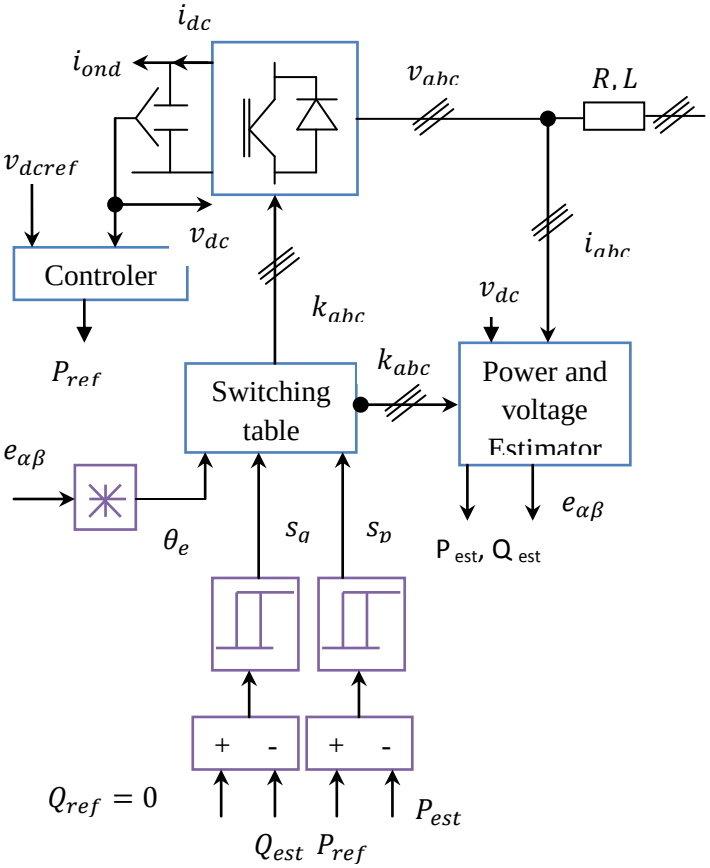

Figure.6. Configuring the DPC for the PWM converter rated network

The Plan sets out the active and reactive instantaneous powers are defined:

$$\begin{bmatrix} P \\ Q \end{bmatrix} = \begin{bmatrix} e_\alpha & e_\beta \\ e_\beta & -e_\alpha \end{bmatrix} \begin{bmatrix} i_\alpha \\ i_\beta \end{bmatrix} \quad (27)$$

As a first approximation, and if the switching frequency is high enough, the change in voltage can be neglected. The variation of active and reactive power can be estimated for the control cycle as follows:

$$\begin{cases} \Delta P = e_\alpha(k).\Delta i_\alpha + e_\beta(k).\Delta i_\beta \\ \Delta Q = e_\beta(k).\Delta i_\alpha - e_\alpha(k).\Delta i_\beta \end{cases} \quad (28)$$

The change of active power and reactive depends on the choice of the voltage vector PWM used. For the seven possible configurations of the converter voltage vector PWM leads to seven possible values of change and reactive power. Consequently, there are different ways of selecting the switching state corresponding to the evolution of control and reactive power. The voltage vector can be expressed in the plan sets as follows:

$$e_{\alpha\beta} = \begin{bmatrix} e_\alpha \\ e_\beta \end{bmatrix} = \sqrt{\frac{2}{3}} \begin{bmatrix} 1 & -1/2 & -1/2 \\ 0 & \sqrt{3}/2 & -\sqrt{3}/2 \end{bmatrix} \begin{bmatrix} e_a \\ e_b \\ e_c \end{bmatrix} \quad (29)$$

With

$e_\alpha = E.\cos(\theta), e_\beta = E.\sin(\theta)$ and $\|e_{\alpha\beta}\| = E$

$-\pi/6 \le \theta \le 11\pi/6$

Where E is the rms line voltage and is the angular position of voltage vector. For smooth operation voltage sensor DPC phase of the converter, the active and reactive powers are estimated using the switching converter, the three phase currents, the DC bus voltage inductance L. They can be derived as follows:

$$\hat{p} = L\left(\frac{di_a}{dt}i_a + \frac{di_b}{dt}i_b + \frac{di_c}{dt}i_c\right) + V_{dc}(S_a i_a + S_b i_b + S_c i_c) \quad (30)$$

$$\hat{q} = \sqrt{3}L\left(\frac{di_a}{dt}i_c - \frac{di_c}{dt}i_a\right) - \frac{1}{\sqrt{3}}V_{dc}[S_a(i_b - i_c) + S_b(i_c - i_a) + S_c(i_a - i_b)] \quad (31)$$

After estimating the instantaneous active and reactive power, the voltage vector can be estimated using the following equation:

$$\begin{bmatrix} \hat{e}_\alpha \\ \hat{e}_\beta \end{bmatrix} = \frac{1}{i_\alpha^2 + i_\beta^2} \begin{bmatrix} i_\alpha & -i_\beta \\ i_\beta & i_\alpha \end{bmatrix} \begin{bmatrix} \hat{p} \\ \hat{q} \end{bmatrix} \quad (32)$$

Sp	Sq	θ1	θ2	θ3	θ4	θ5	θ6	θ7	θ8	θ9	θ10	θ11	θ12
1	0	V_5	V_6	V_6	V_1	V_1	V_2	V_2	V_3	V_3	V_4	V_4	V_5
0	1	V_3	V_4	V_4	V_5	V_5	V_6	V_6	V_1	V_1	V_2	V_2	V_3
	0	V_6	V_1	V_1	V_2	V_2	V_3	V_3	V_4	V_4	V_5	V_5	V_6
	1	V_1	V_2	V_2	V_3	V_3	V_4	V_4	V_5	V_5	V_6	V_6	V_1

Table .2.The new switching table for DPC

4.2. Setting the DC bus voltage

In this work, setting the DC bus voltage is provided by a proportional integrator (PI), the latter can provide the reference of active power. The reference reactive power is zero imposed to ensure a functioning unity power factor.

System figure 7 is modeled by the following equation:

$$\frac{1}{C}\int_0^t V_{dc}.dt = I_{dc} - I_{ond} \quad (33)$$

The transfer function of PI controller is written as follows:

$$F(s) = \frac{1 + k_p Ts}{T_i s} \quad avec \quad \frac{1}{T_i} = k_i \quad (34)$$

4.3. Simulation Results

The platform of Matlab / Simulink was used to simulate the complete model of the wind conversion chain (7.5KW), the results obtained allow one hand to analyze the various quantities characterizing the cascade constituting the two PWM converters and secondly, bring up the performance obtained by the two commands used DTC (rotor side) and DPC (network side).

Figure 8 shows the electromagnetic torque and its reference generated by the algorithm (MPPT), the latter reacts significantly to changes in wind speed, the rotor flux with the reference1.60Weber.

Figure 9 shows the active and reactive power transited to the grid with their references, current and phase voltage. Through these values, we find that the command has focused DPC system dynamics very important and satisfactory operation.

Figure 10 shows the variation of the DC bus and the benchmark. We note that it has a dynamic fast enough around its reference.

Figure 11 shows that the currents of the rotor and stator respectively are sinusoidal but of different frequency

5. Conclusion

In this paper, we presented two techniques to control DTC (Direct Torque Control) and DPC (Direct Power Control) system applied to the conversion of wind energy based on the machine has dual power (DFIG). This machine is designed to produce electrical energy; it is useful to think in terms of power or torque, to the DTC that is developed in this work. An algorithm for maximizing power (MPPT) has been implemented; it is to enslave the speed of the machine by a sliding mode controller with a particular reference optimally corresponds to a maximum power coefficient. The CPD is used to control the grid side PWM converter, the latter is based on two references of active and reactive power. The reference active power is obtained by the control DC bus (using the PI controller) with its reference 617V and the reference reactive power is zero imposed to ensure operation at unity power factor.

References

[1] S. Muller, et al., "Doubly Fed Induction Generator System for Wind Turbines", IEEE Industry Application Magazine 8(3), pp.26-33, May/June 2002.

[2] Tapia, A. Tapia, G. Ostolaza, J. X. Saenz, J. R., "Modeling And Control Of A Wind Turbine Driven Doubly Fed Induction Generator", IEEE Transactions On Energy Conversion, No. 2 (June 2003), pp. 194–204.

[3] D.Beriber, M.O. Mahmoudi, E.M.Berkouk, A.Talha, "Study And Control Of Tow Level Pwm Rectifiers-Clamping Bridge-Tow Level NPC VSI Cascade. Application Double Stator Induction Machine", IEEE Power Electronics Specialists conference, pp.3894-3899, Aachen Germany, 2004.

[4] A. Chaiba, R. Abdessemed, M. L. Bendaas ,"A Torque Tracking Control Algorithm For Doubly–Fed Induction Generator", Journal Of Electrical Engineering, Vol. 59, N° 3, 2008, pp. 165–168.

[5]L. Honefors, A. Petersson, T. Thiringer And T. Petru., "Modelling And Experimental Verification Of Grid Interaction Of A DFIG Wind Turbine. IEEE Transaction On Energy Conversion. Vol.20, N°.4, pp.878-868, December 2005.

[6] A.Boyette ." Commande d'un Générateur Asynchrone A Double Alimentation avec un Système de Stockage pour la Production Eolienne" .Thèse De Doctorat De L'université Henri Poincaré, Nancy I , (France) 2006.

[7] F.Bouchafaa. "Étude Et Commande De Différentes Cascades A Onduleur A Neuf Niveaux A Structure NPC. Application A La Conduite D'une MSAP". Thèse De Doctorat En Automatique, Ecole Nationale Polytechnique Algeria, 2006.

[8] X.Yao, C. Yi, Deng ying, J. Guo , L.Yang, "The Grid-side PWM Converter of the Wind Power Generation System Based on Fuzzy Sliding Mode Control", International Conference on Advanced Intelligent Mechatronics, Proceedings of the 2008 IEEE/ASME July 2 - 5, 2008, Xi'an, China.

[9] Jun Yao, Hui Li, Yong Liao, and Zhe Chen, "An Improved Control Strategy of Limiting the DC-Link Voltage Fluctuation for a Doubly Fed Induction Wind Generator, IEEE transactions on power electronics, Vol. 23, No. 3, may 2008.

[10] G.salloum. "Contribution a la commande robuste de la machine asynchrone à double alimentation », Thèse de doctorat, Institut National Polytechnique de Toulouse (France), 2007.

[11] Boukhezzar B, Lupu L, Siguerdidjane H, Hand M. Multivariable Control Strategy for Variable Speed, Variable PitchWind Turbines. Renewable Energy International Journal, Elsevier, 2006.

[12] Larrinaga SA, Vidal MAR, Oyarbide E, Apraiz JRT. Predictive control strategy of DC/AC converters based on direct power control. IEEE Trans Ind Electron 2007; 54(3):1261–71.

[13] V.I Utkin, _Sliding mode control design principles and applications to electric drives_, IEEE Trans, on Industrial Electronics, Vol.40, No.1, February 1993, pp.23-36.

[14] Y.P. Obulesu, M.V.Kumar, "Design and simulation of direct torque control of Induction Motor drive using Matlab/Simulink," International Journal of Power and Energy Systems, Vol. 27, No.2, 2007.

[15] F. Blaabjerg, F. Iov, Z. Chen, and R. Teodorescu, "Power electronics in renewable energy systems," Keynote paper at EPE-PEMC 2006

Conference, August 30 - September 1 2006, Portoroz , Slovenia, p.17, IEEE Catalog Number: 06EX1405C, ISBN 1-4244-0449-5.
[16] R. Teodorescu, F. Iov, F. Blaabjerg"Modeling and control of grid converter. Phase 1a:Basic grid inverter control" February 2006.

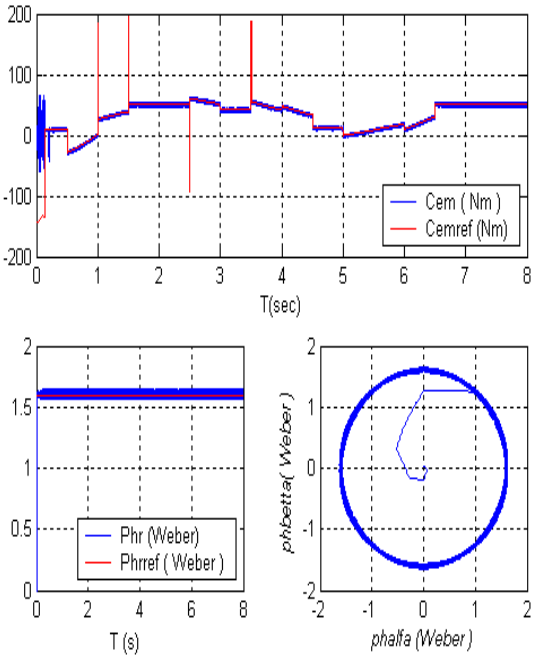

Figure .7.Torque and rotor flux

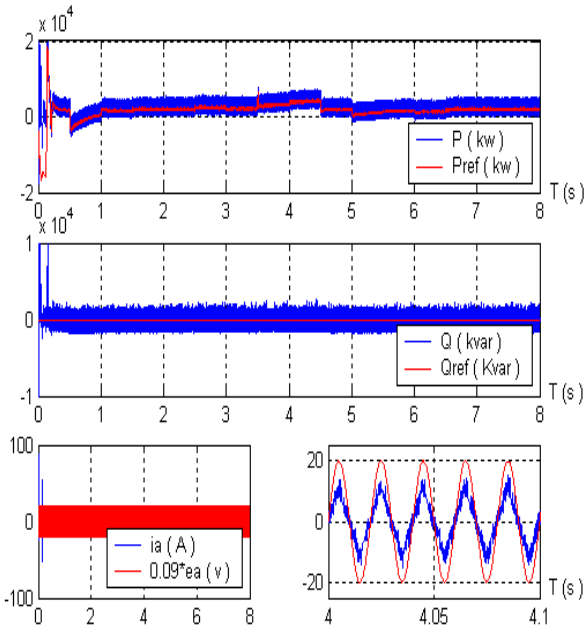

Figure .8.Power (active, reactive) and current-voltage phase

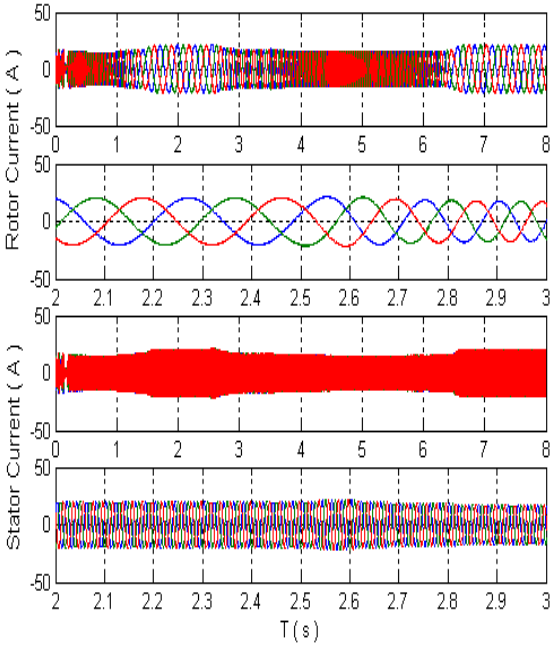

Figure .9.Phase currents rotor and stator

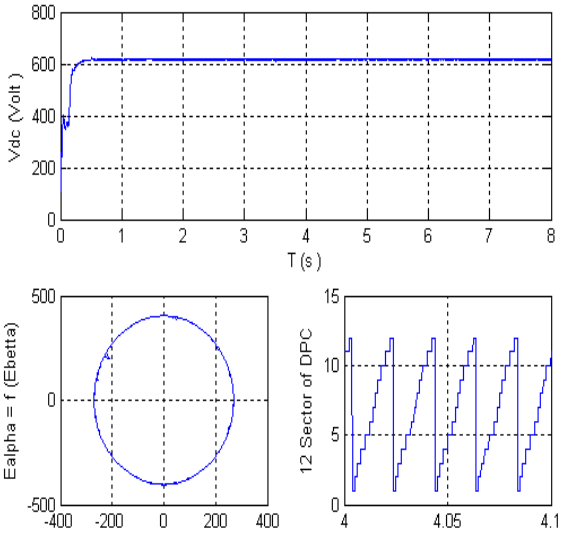

Figure .10.DC bus voltage and sector